Evidence for a System of Planets Orbiting Upsilon Andromedae

S.G. Korzennik[1], R.W. Noyes[1], P. Nisenson[1], M.J. Holman[1], A. Contos[1], and T.M. Brown[2]

(1) Harvard-Smithsonian Center for Astrophysics, Cambridge, MA, U.S.A.
(2) High Altitude Observatory, NCAR, Boulder, CO, U.S.A.

SUMMARY

Using the Advanced Fiber Optic Echelle (AFOE) spectrograph at SAO's Whipple Observatory, we have monitored the radial velocity of Upsilon Andromedae since September 1994.
The AFOE data show:

- The already known close-in "hot Jupiter" in a 4.6-day circular orbit.
- A middle companion with a well-defined 243.5 day orbit and orbital parameters in close agreement with Lick.
- An outer companion with an orbit between 1200 and 1500 days — (not well-determined because the total observing span encompasses only about one period).

Independent results from two different groups with different instruments and analysis methodologies makes it highly likely that a true planetary "system" has now been discovered around a star like our own.
Numerical integrations show:

- The system can be stable, but only for certain combinations of periods, masses, and eccentricities of the outer two companions.
- The stability requirement imposes an upper limit on the actual planetary masses, and on the difference in orbital inclination of the two outer planets.
- The longitudes of periastron of the two outer companions may be locked to nearly the same value, matching the observations.

The Advanced Fiber Optic Echelle (AFOE)

- A joint project of SAO and HAO. The instrument is located at the 1.5-m telescope of the Whipple Observatory at Mt. Hopkins, AZ; and has the goal to measure stellar radial velocities to a precision of a few m/s.
- The method: Use a fiber-fed 2-D echelle spectrograph with $R \sim 50{,}000$ (Brown *et al*, 1994). An I_2 cell is placed in the beam path to provide a stable wavelength standard.

Observations and Data Analysis

Introduction

- Observations started September 1994; intensified in 1996 after close-in companion announced (Butler *et al*, 1997).
- Figure 1 shows raw AFOE (red) and Lick (green) data, data after subtracting best fits for the close-in companion, and after additionally subtracting best fits for a long-period (3.5 year for Lick, 4.0 year for AFOE) companion. The latter residual plot shows evidence for a companion with intermediate period around 240 days.
- **CONCLUSION:** The AFOE data, both independently and when combined with Lick data, gives evidence for three companions to Upsilon Andromedae, which we label "b", "c", and "d" in order of increasing semi-major axis.

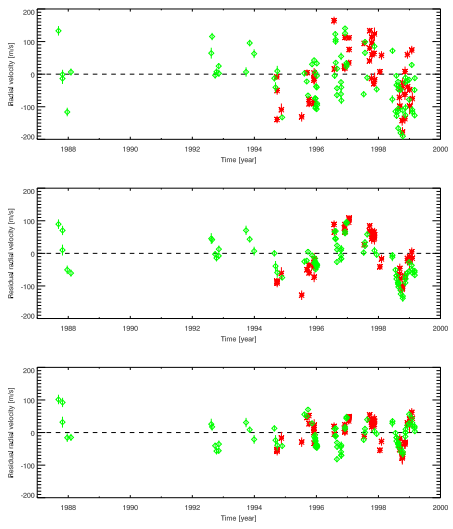

Figure 1: *Top panel: Radial velocity observations of upsilon Andromedae, with the AFOE (red) from September 1994 to January 1999, and by the Lick group (green).*
Middle panel: residual velocities after subtracting the Keplerian orbital fit to the close-in companion.
Bottom panel: residual velocities after subtracting Keplerian orbital fits to the both the close-in and distant companions.

Analysis

AFOE data (52 points) were analyzed independently, and in combination with the Lick data (89 points). Each data set was modelled as the sum of three Keplerians. Resulting orbital parameters (including the fit to the Lick data independently) are given in Table 1 (cf. Butler *et al*, 1999, submitted).

Table 1

Parameters	Lick data	AFOE data	Combined Lick/AFOE
Companion "b"			
P (d)	4.6171 ± 0.0001	4.6171 ± 0.0003	4.6170 ± 0.0003
T_{peri} (JD)	2450315.34 ± 0.7	2450001.99 ± 0.51	2450002.24 ± 3.1
e	0.042 ± 0.030	0.042 ± 0.033	0.034 ± 0.15
ω (deg)	16.0 ± 139	63.8 ± 40	83.0 ± 243
K_1 (m s^{-1})	74.5 ± 2.3	75.6 ± 2.3	73.0 ± 5
$a_1 \sin i$ (AU)	3.16×10^{-5}	3.21×10^{-5}	3.10×10^{-5}
a_b (AU)	0.059	0.059	0.059
$M_b \sin i$ (M_{JUP})	0.72	0.74	0.71
Companion "c"			
P (d)	242.0 ± 0.7	243.5 ± 1.0	241.2 ± 1.1
T_{peri} (JD)	2451131.24 ± 23.4	2450140.4 ± 8.3	2450154.9 ± 20.8
e	0.23 ± 0.06	0.22 ± 0.06	0.18 ± 0.11
ω (deg)	261.0 ± 47	219.2 ± 14	243.6 ± 33
K_1 (m s^{-1})	56.0 ± 2.5	53.7 ± 3.5	58.0 ± 7.9
$a_1 \sin i$ (AU)	0.0012	0.0012	0.0013
a_c (AU)	0.83	0.83	0.83
$M_c \sin i$ (M_{JUP})	1.98	1.96	2.11
Companion "d"			
P (d)	1269.0 ± 8.5	1481.2 ± 35	1266.6 ± 30
T_{peri} (JD)	2453813.46 ± 32.0	2450046.8 ± 16.1	2451308.7 ± 40.5
e	0.36 ± 0.05	0.44 ± 0.05	0.41 ± 0.11
ω (deg)	236.0 ± 14.6	245.9 ± 5.9	247.7 ± 17.0
K_1 (m s^{-1})	69.5 ± 2.1	85.5 ± 4.0	72.9 ± 7.1
$a_1 \sin i$ (AU)	0.0076	0.0105	0.0077
a_d (AU)	2.50	2.78	2.50
$M_d \sin i$ (M_{JUP})	4.11	5.70	4.61
N(obs)	89	52	141
RMS resid.	15.12	12.1	18.7

Companion "b"

- Figure 2 shows partial phase plots for companion "b", *i.e.* velocity residuals after subtracting fits for "c" and "d", phased according to the period and phase of "b" determined from the combined data. Also shown are periodograms of those residuals, for both the individual data sets and the combined data.
- **CONCLUSION:** The orbital properties of the (already known) inner companion are found to be essentially identical in the AFOE, Lick, and combined data sets (see also Table 1).

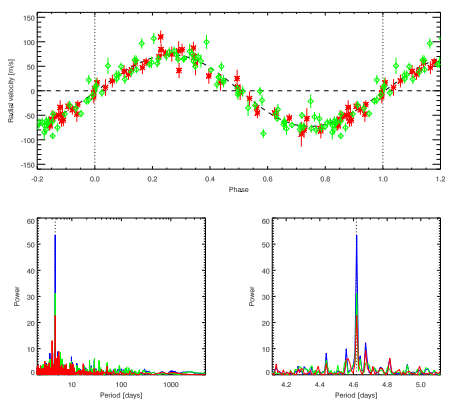

Figure 2: *Top panel: Partial phase plot for companion "b", i.e., residual velocities after subtracting the Keplerian orbital fit for companions "c" and "d". The AFOE observations are plotted in red, the Lick observations in green.*
Botton panels: Periodograms of the residual velocities shown in the top panel, for the AFOE data only (red), Lick data only (green) and combined data (blue).

Companion "c"

- Figure 3a shows partial phase plots for companion "c", i.e. velocity residuals after subtracting fits for "b" and "d", phased according to the period and phase of "c" determined from the combined data. Also shown are periodograms of those residuals, for both the individual data sets and the combined data. The halfwidth of the AFOE periodogram peak data alone is broader than that for the Lick or combined data, because of the shorter time span of the AFOE data. The significance of the peak in the combined data is substantially greater than for either data set alone.
- **CONCLUSION:** The Lick and AFOE data sets provide a mutually confirming positive detection of companion "c", and together reveal the first sunlike star (other than the Sun) with several planetary companions. As for companion "b", all orbital parameters agree within their uncertainties (Table 1).

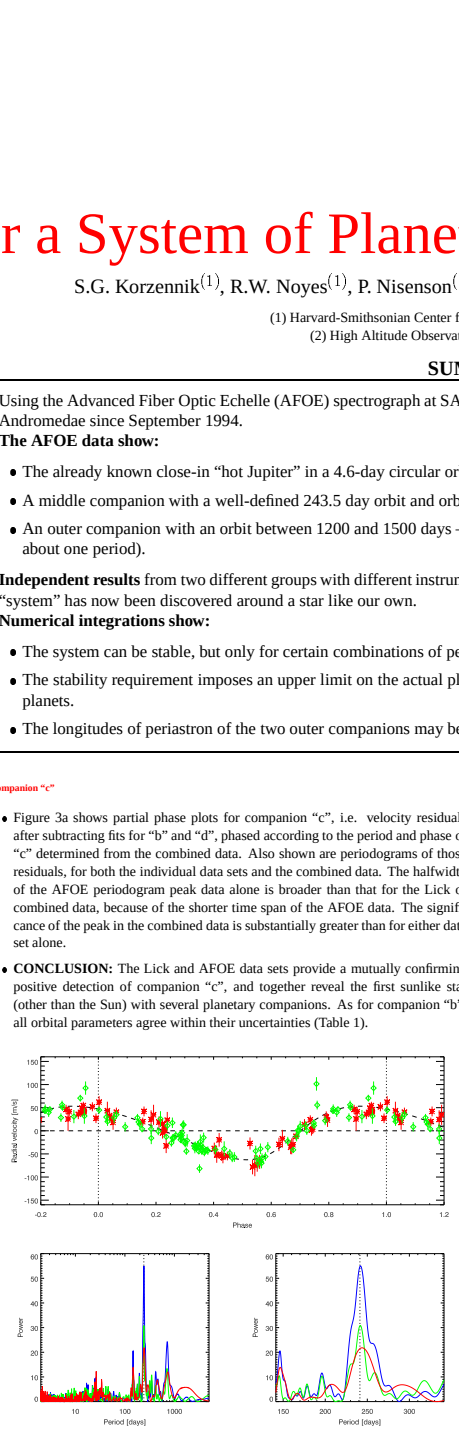

Figure 3: *Top panel: Partial phase plot for companion "c", i.e., residual velocities after subtracting the Keplerian orbital fit for companions "b" and "d". The AFOE observations are plotted in red, the Lick observations in green.*
Botton panels: Periodograms of the residual velocities shown in the top panel, for the AFOE data only (red), Lick data only (green) and combined data (blue).

Companion "d"

- Figure 4a shows residuals to the AFOE and Lick data (red and green respectively), after subtracting the individual fits for "b" and "c". The two residuals track each other well, except for an apparently systematic offset in 1997 and 1998 which is not yet resolved. The period of "d" is not well-constrained by either data set, because of uneven sampling and (for the AFOE data) a relatively short observing span.
- Figure 4b shows periodograms of the residuals to the AFOE, Lick, and combined data after subtracting the corresponding fits for "b" and "c". The breadth of the periodogram peaks near 1300 days illustrates that the period of "d" is not well determined from the data. The "best-fit" periods for "d" derived from 3-Keplerian fits to these data sets are shown by the dashed red, green, and blue vertical lines. Because of the significant eccentricity of "d", these "best-fit" periods do not lie at the maximum value of the corresponding periodograms.

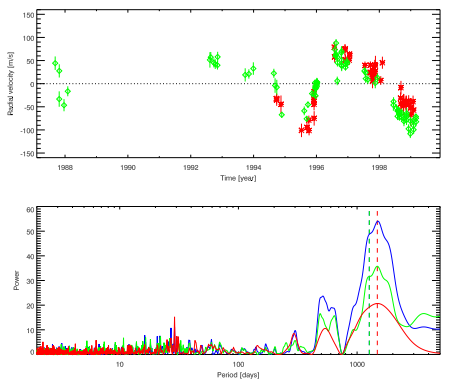

Figure 4: *Top panel: Residual velocities after subtracting the Keplerian orbital fit for companions "b" and "c". The AFOE observations are plotted in red, the Lick observations in green.*
Bottom panel: Periodograms of the residual velocities shown in the top panel, for the AFOE data only (red), Lick data only (green) and combined data (blue). Vertical lines show periods from best 3-Keplerian fits to raw data.

- Figure 5 shows the same data as in 4a, but with the orbital fits for "d" derived from the AFOE, Lick, and combined data superimposed. It illustrates once again that the period of "d" is not well-constrained.

  However, in coming months the velocity due to "d" should rise steeply if its parameters are like those of the Lick or combined data, but should continue falling if they are like those of the AFOE data. Thus, observations over the next few months may yield a much better constrained value for the period.

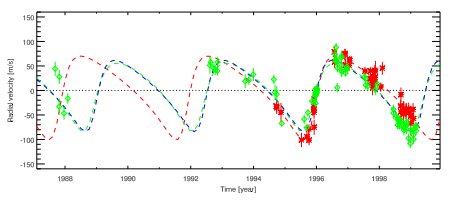

Figure 5: *Residual velocities after subtracting the Keplerian orbital fit for companions "b" and "c". The AFOE observations are plotted in red, the Lick observations in green. The orbital fits for companion "d" based on the AFOE, Lick, and combined data sets are shown as red, green and blue dashed lines.*

- **CONCLUSION:** Companion "d" is seen in both data sets, although its period (semi-major axis) and eccentricity are not yet well-defined. Note (see Table 1) that both data sets give the same value of periastron angle ω, and that this value is approximately the same as for companion "c" (see discussion below).

Other Companions?

- Figure 6a shows the residuals to the AFOE (red) and Lick (green) data sets after subtraction of the corresponding orbital fits for all three companions. Figure 6b shows the corresponding periodograms. This illustrates that neither data set shows evidence for additional periodic velocity variations in the data.

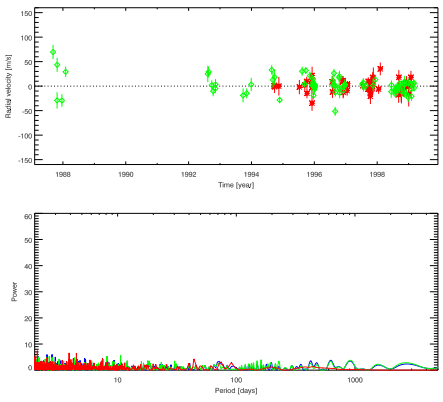

Figure 6: *Top panel: Residual velocities after subtracting the Keplerian orbital fit for all 3 companions. The AFOE observations are plotted in red, the Lick observations in green.*
Botton panel: Periodograms of the residual velocities, after subtracting the Keplerian orbital fits for all 3 companions.

Orbital Stability Calculations

Approach

- Upsilon Andromedae is about 2.6 Gy old, so the system must be stable on that time scale. This provides constraints on orbital elements, and on actual masses. (Data yield only minimum mass $m \sin i$, where i is orbital inclination.)
- We explore system stability using symplectic n-body integrations (Wisdom and Holman 1991), which are fully 3-d and include all gravitational interactions including general relativistic (GR) precession.
- GR precession of "b" is faster than its precession due to interactions with the other companions, and thus prevents large eccentricity oscillations induced by the latter, which otherwise might lead to instability (cf. Lissauer 1999)
- Result: the eccentricity oscillations of "b" remain small enough so as not to contribute to system instability (see Figure 7). Therefore, "b" can be ignored in system stability calculations, thus speeding up the integrations. Comparative integrations of two and three-planet models for the Upsilon Andromedae system have been carried out and validate this approach.

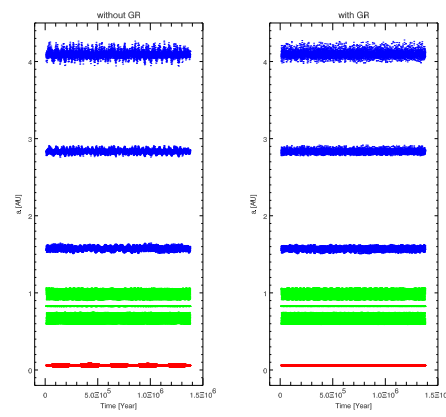

Figure 7: *Time evolution of periastron, semi-major axis, and apastron, for "b", "c", and "d" (red, green, and blue respectively). In the left panel calculations, which do not include GR precession, the eccentricity of "b" periodically grows as large as 0.42. In the right panel calculations, which include GR precession, the eccentricity remains no larger than 0.08. The quasi-periodic structure in the orbit of "d", seen in the left panel, disappears when GR precession is included.*

Calculations

- Since orbital elements of "c" are well characterized by observations, we vary the less well-determined semi-major axis and eccentricity of "d" to find which values lead to instability.
- We also carry out calculations for different mass factor $\mu = 1/\sin i$, (where the orbital inclination i is assumed approximately the same for "c" and "d"), to find how the domain of stability changes for planetary masses larger than the minimum masses (*i.e.*, for $\sin i = 1$.)
- Figure 8a shows regions of stability (light) and instability (dark) as a function of semi-major axis a_d and eccentricity e_d of companion "d", for mass factor $\mu = 1$. Note "fingers" of instability extending to lower eccentricity near values of a_d (2.13, 2.30, 2.45, 2.61, 2.76 AU) corresponding to mean motion resonances—values of a_d at which the orbital periods of "c" and "d" are commensurate. These stability calculations extend to 10^7 years.
- Figure 8b shows a more detailed calculation of the region Figure 8a near the combined-fit parameters for "d". These calculations were carried out on a finer grid, and extended to 10^8 years. The position of the instability/stability boundary does not change significantly with longer integrations. Note that the system with combined-data fit parameters (a_d = 2.50 AU, e_d = 0.41) is stable, although it would be unstable, for example, for a_d = 2.45 AU.
- Figure 8c is similar to Figure 8a, but corresponds to a mass factor $\mu = 2.0$ ($i = 30°$). Note that the boundary between stability and instability has shifted to smaller values of eccentricity. The best fit for the combined data is now unstable, and the Lick fit nearly so.

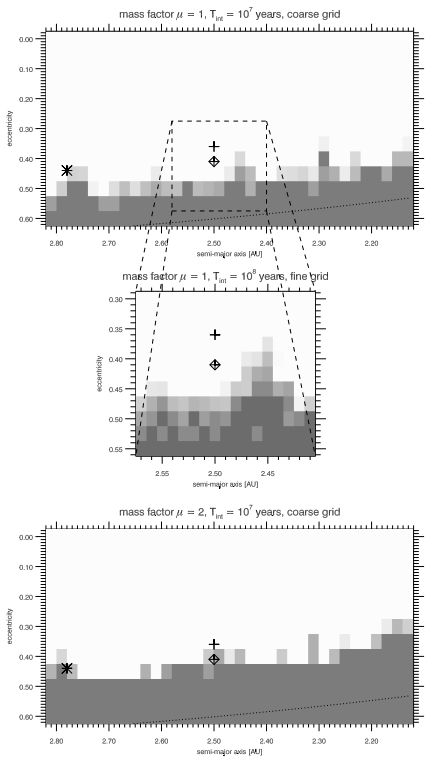

Figure 8: *Stability calculation results as a function of a_d, e_d. Light regions are stable, dark unstable. Crosses, diamonds, and stars indicate location of best fits to Lick, combined, and AFOE data respectively. Top: Mass factor $\mu = 1.0$. Calculations extend to 10^7 years. Middle: $\mu = 1.0$, region near best fit to combined data, on finer grid and with calculations extending to 10^8 years. Bottom: As in top panel, except $\mu = 2.0$.*

The Stability/Instability Boundary in 3 Dimensions

- Figure 9 shows how the boundary between stability and instability depends on the 3 parameters a_d, e_d, and μ. Stable regions are rendered opaque and red, unstable regions are transparent (or blue at the edges). The boundary surface (yellow) is convoluted, but sharp and well-defined.
- The location of the best fits to the AFOE, combined, and Lick data sets are shown (left to right) in Figure 9 as purple vertical lines. They disappear from view at the mass factors (μ = 1.2, 1.6, and 2.1 respectively) below which the orbits are stable.
- **CONCLUSION:** A more accurate observational determination of a_d and e_d (expected soon; see above) may put significantly tighter constraints on the minimum mass of the planetary system than currently provided by Hipparcos data (which imply only that $\mu \leq 2.5$).

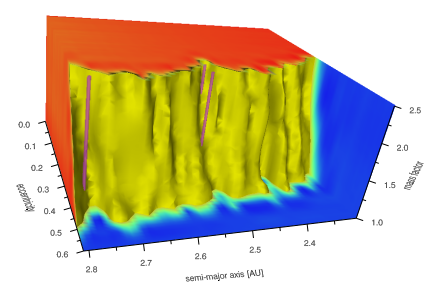

Figure 9: *Regions of stability (opaque/red) and instability (transparent/blue) as a function of a_d (increasing right to left), e_d (increasing back to front), and μ (increasing bottom to top). The yellow-green surface marks the boundary between unstable and stable regions. The three purple columns, in order from left to right in this view, mark the values of a_d and e_d for the AFOE, Lick, and combined-data solutions respectively. They disappear within the stable region at the value of μ (1.2, 1.6, and 2.1) below which the respective solutions are stable.*

Mutual Inclination of Orbits

- The inclination between the orbits of "c" and "d" is also constrained by instability criteria.
- Preliminary calculations were made for the combined-data solution, leaving the masses as given in Table 1, but changing the relative inclination of "c" and "d". The system was found to be is stable at a relative inclination of 30°, but unstable at a relative inclination of 60°. This is consistent with known analytical results (Kozai 1962) that the transition should occur near 42°.

Phase-locking of Longitudes of Periastron?

- The longitudes ω of periastron of "c" and "d" are the same within observational uncertainties. Is this just coincidence?
- We have begun calculations of the variation of the difference $\delta\omega_{c,d} = \omega_d - \omega_c$ as a function of time, depending on starting values of this difference. We find, for the a_d and e_d given by the combined data set, and mass factor $\mu = 1$, that for initial values of $|\,\delta\omega_{c,d}\,|$ less than about 45 degrees, $|\,\delta\omega_{c,d}\,|$ remains within that range. Conversely, for larger initial values of $|\,\delta\omega_{c,d}\,|$, $\delta\omega_{c,d}$ samples all angles.
- A possible implication is that the periastron angles of "c" and "d" are locked together by a secular resonance. Further investigations are under way. If this is true, it may give clues to the formation and early evolution of the Upsilon Andromedae system.

Acknowledgements

This work was supported by NASA, NSF, and the Smithsonian Institution.

References

Brown, T. M., Noyes, R. W., Nisenson, P., Korzennik, S. G., Horner, S. D. 1994, PASP, 106, 1285.

Butler, R. P., Marcy, G. W., Williams, E., Hauser, H., & Shirts, P. 1997, ApJ, 474, L115.

Butler, R. P., Marcy, G. W., Fischer, D.A., Brown, T. M., Contos, A. R., Korzennik, S. G., Nisenson, P., & Noyes, R. W. 1999, Ap. J. *submitted.*

Kozai, Y. 1962, Astron. J. 67, 591.

Lissauer, J. J. 1999, Nature, 398, 659.

Wisdom, J. & Holman, M. 1991, Astron. J. 102, 1528.